Effects of bottom gap in confined space on the critical heat flux under pool-boiling condition

Seong Ho Kim [a], Koung Moon Kim [a, b], Ho seon Ahn [a, b, c *]
[a] *Department of Mechanical Engineering, Incheon National University, Incheon, Republic of Korea*
[b] *Nuclear Safety Research Institute, Incheon National University, Incheon, Republic of Korea*
[c] *AHN Materials Inc., Incheon, Republic of Korea*
[*] *Corresponding author: hsahn@inu.ac.kr*

1. Introduction

In previous research, it has been reported that the critical heat flux (CHF) is affected by various factors such as vertical and horizontal surface orientation [1], wettability, roughness, and morphology of the boiling surface [2-5]. In narrowed flow path, CHF could decrease due to the vapor bubble blocking by the increased drag force. In our previous research [6], it was investigated the effect of the confined flow path near the horizontal heater on the boiling heat transfer in terms of CHF (Fig. 1).

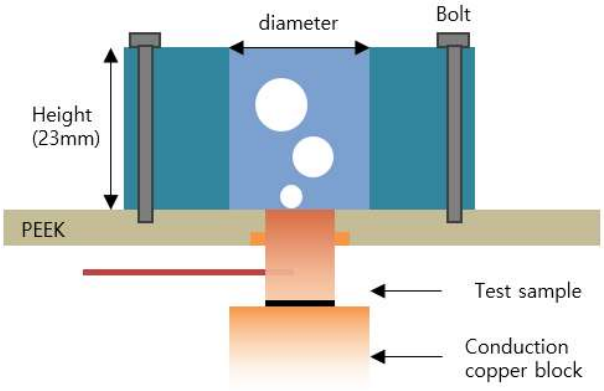

Figure 1 Vertically confined flow path by constructing the cylindrical wall

It was reported that CHF performance can be improved even in a very narrow flow path with a gap of 1 mm between the vertical wall and the circular heater.

The present study is the follow-up research to investigate the effect of the coolant supplement nearest the heater. To investigate this effect, the horizontal disk combined the vertically confined cylinder for constructing the coolant flow path in the horizontal direction as shown in Fig 2.

Nomenclature

D_c	Cylindrical wall inner diameter [mm]
H_c	Cylindrical wall height [mm]
B	Bottom gap [mm]
q''	Heat flux [kW/m^2]
k	Thermal conductivity [kW/m·K]
T_{sur}	Test sample surface temperature [K]
$T_0 \sim T_3$	Measured temperature at each point [K]
d	distance of surface and T_0 point [mm]
Δx	Axial distance [mm]

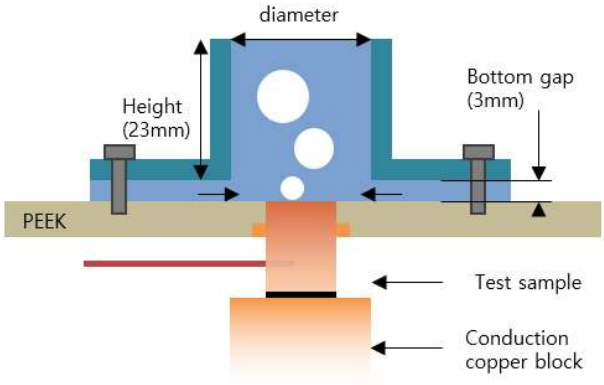

Figure 2 Vertically and horizontal confined flow path by constructing the cylindrical wall

2. Experimental apparatus and procedure

This section is presented the experimental apparatus consisting of a pool, copper block, conduction copper block and test sample. Next it is presented that cylindrical wall setup and the experimental procedure.

2.1 Experimental apparatus and acquisition data

Figure 3 shows a schematic apparatus consisting of a boiling pool, a copper blocks, a test sample and confined cylindrical wall. The boiling pool has immersion cartridge heater, visualization windows, and a reflux condenser. Boiling pool size is 150 x 150 x 230 mm and made of aluminum alloy. Front and back side has visualization window made of polycarbonate and that thickness is 10mm. The immersion cartridge heater of 700W was installed to keep the working fluid (distilled water) saturated condition in the pool. The reflux condenser was installed top of the boiling pool. And installed reflux condenser converted steam back into water.

As shown in Figure 3, the test sample was located at the bottom of the pool. During the boiling experiments, the test sample is heated through the conduction heat transfer from the heating section in the copper block. Copper block has 10 cartridge heaters, and each heater has 350W. The cartridge heaters heat up the copper block, and that heat is transferred to conduction copper block. So heated conduction copper block's heat is transferred

to test sample through the one dimensional conduction. Between conduction copper block and test sample, there was a thin graphite sheet to reduce the thermal contact resistance.

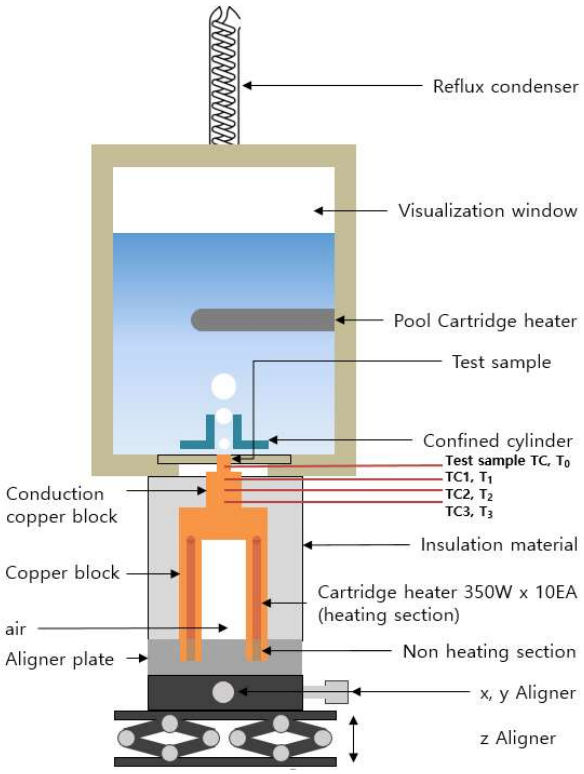

Figure 3 experimental apparatus

As shown in Figure 3, the test sample in present study is made by horizontal and circular copper and side wall of the test sample is insulated by Polyether ether ketone (PEEK). Conduction

copper block connected three 1mm O.D K-type thermocouples (TC) and each TC interval is 8mm in order to calculate the temperature difference and heat flux. Assuming a one dimensional steady – state condition, the heat flux is calculated using the conduction heat transfer equation.

$$q'' = k \times \frac{\Delta T}{\Delta x} = k \times \frac{T_2 - T_1}{\Delta x} \quad (1)$$

Where T_1 and T_2 are the measured temperature, q'' is calculated heat flux. The linearity of the measurement temperature in the conduction copper block was evaluated by commercial software, Fluent 6.0 in previous study [7]. So calculated heat flux is reliable.

$$\Delta T_{sur} = T_{sur} - T_{sat} = \left(T_0 - \frac{q''}{k} d \right) - T_{sat} \quad (2)$$

Surface temperature also can calculated with equation (2). The data acquisition system (HP – Agilent, 34970A) measured all temperatures at intervals of one second.

2.2 cylindrical wall setup

Figure 1 shows the setup of a cylindrical wall made of high – density polyethylene around the test sample. The outer diameter of the cylindrical wall is fixed at 50mm and the height is 23mm. silicon sealant was applied between the PEEK and cylindrical wall in order to block the distilled water (DI – water).

Figure 2 show the setup of a cylindrical wall made of polycarbonate around the test sample. Wall thickness is 1.5mm and height is 23mm. The different from Figure 1 is that the bottom of the cylindrical wall has 3mm gap on the test sample. Various cylindrical wall inner diameter were used in the experiment.

2.3 experiment procedure

After aligning the x and y axes used by x, y aligners, the test sample and the conduction copper block were connected using z aligner. The pool is filled with DI – water and it was saturated to the atmospheric pressure condition by the pool cartridge heater. Through the reflux condenser, the water volume was maintained with 3L. After the DI – water saturation in the pool, the copper block started to heat the test sample. All acquisition temperature data were averaged with 3 min intervals with the heat flux and the surface temperature as Equations (1) and (2). When CHF occurs on the test sample, the test sample and conduction copper block were detached immediately using z aligner. This behavior protected the test sample from thermal damage during CHF.

3. Results and Conclusions

In this experiment, the bottom gap and cylindrical wall height were fixed 3mm and 23mm, respectively. The conducted experimental cases were 7, 12, 17, 22, and 27mm of the cylindrical wall inner diameters. Figure 4 shows the present experimental result with comparing the previous results in Ref. [6]. In previous results, CHF performance in the case of 30 mm was similar to that of the bare case because the diameter was too large to affect CHF performance. Contrastively, CHF performance was diminished dramatically in the case of 8 mm compared to that of the bare case due to the disturbance of the bubble escape and decreased coolant supplement due to the narrowed flow path. In the case of 10 mm, CHF performance was improved by optimizing the escape of vapor bubbles and the supply of coolant in the appropriately narrowed flow path.

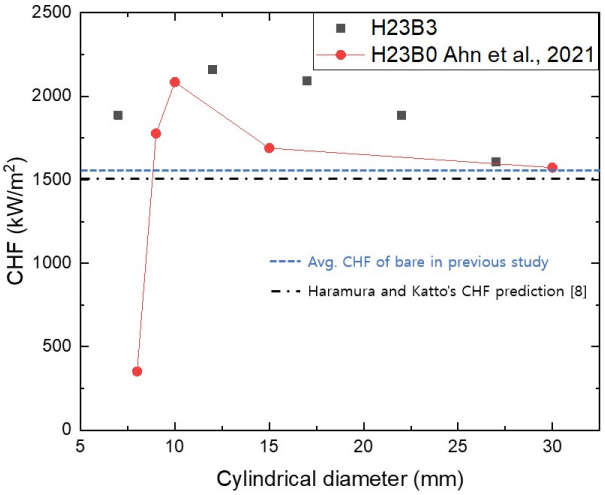

Figure 4 CHF versus D_c with different B

In the present experimental result, CHF performance is similar to the bare in the case of the 27 mm. However, CHF performances are improved in the other cases. In addition, CHF performance is not degraded ever for the case of the 7 mm, which is smaller than the heater diameter. From these results, we can predict the coolant supplement near the heater in the horizontal direction can enhance the heat transfer performance. As the confined wall diameter decreased from 27 mm to 12 mm, CHF increases. As the diameter decreases, it can be predicted that the coolant supply in the horizontal direction is accelerated by increasing the velocity of the escaping vapor bubble. Although CHF decreases slightly in the case of 7 mm, the drastic decrease in CHF can be prevented by supplying coolant near the heater compared to the previous research result.

For further research, we are conducting the high-speed visualization in order to clarify the liquid inflow effect though the gap.

Acknowledgments

This research was supported by National Research Foundation in Korea (NRF-2020R1F1A1051374).

REFERENCES

[1] J.M. Kim, J.H. Kim, H.S. Ahn, Hydrodynamics of nucleate boiling on downward surface with various orientation. Part I: Departure diameter, frequency, and escape speed of the slug, Int. J. Heat Mass Transfer 116 (2018) 1341–1351.
[2] H.S. Ahn, H.J. Jo, S.H. Kang, M.H. Kim, Effect of liquid spreading due to nano/micro structures on the critical heat flux during pool boiling, Applied Physics Letters, 98, 071908 (2011)
[3] H.S. Ahn, C. Lee, J.W. Kim, M.W. Kim, The effect of capillary wicking action of micro/nano structures on pool boiling critical heat flux, Int J. Heat and Mass Transfer 55 (2012) 89-92.
[4] Harry O'Hanley et al, Separate effects of surface roughness, wettability, and porosity on the boiling critical heat flux, Applied Physics Letters 103, 024102 (2013).
[5] J.S. Kim, S.C. Jun, L. Ram, S.M. You, Effect of surface roughness on pool boiling heat transfer at a heated surface having moderate wettability, Int J. Heat and Mass Transfer 101 (2016) 992-1002.
[6] H.S. Ahn, K. M. Kim, S. Wongwises, D. W. Jerng, Effects of confined space on the critical heat flux under the pool – boiling condition, Alexandria Engineering Journal, 2021.
[7] H.S. Ahn, H. Kim, H.J. Jo, S.H. Kang W.P. Chang, M.H. Kim, Experimental study of critical heat flux enhancement during force convective flow boiling of nanofluid on a short heated surface, Int J. Multiph, Flow 36 (2010) 375-384.
[8] Y. Haramura, Y. Katto, A new hydrodynamic model of the critical heat flux, applicable widely to both pool and forced convective boiling on submerged bodies in saturated liquids, Int. J. Heat Mass Transf. 26 (1983) 389–399.